Quantum Heisenberg Spin Chains with Inversely Linear Correlated Disorder: Localization Effects and State Transfer Protocols

Marconi Silva Santos Junior[1], Messias de Oliveira Sales[2], Guilherme M A Almeida[1] and Francisco Anacleto Barros Fidelis de Moura[1]

1) Instituto de Física, Universidade Federal de Alagoas, Maceió AL 57072-970, Brazil

2) IFMA Campus São João dos Patos, Rua Padre Santiago, n 100, Santiago, São João dos Patos-MA, 65665-000, Brazil

December 9, 2024

Abstract

In this work, we investigate the effects of correlated disorder on the quantum Heisenberg spin chain. The exchange couplings between adjacent spins are modeled as a disordered distribution with inverse linear correlation function controlled by a parameter γ. The Cholesky decomposition method is employed to generate the spin-spin coupling that adheres to this correlation structure. By analyzing the autocorrelation function, we observe the influence of the correlation parameter γ on the decay behavior of the autocorrelation. Furthermore, we study the eigenstates of the Hamiltonian in the one-magnon subspace and calculate the density of states and the participation ratio, providing insights into the localization properties of the system. Our findings suggest that introducing correlated disorder significantly alters the physical properties of the spin chain, which could have implications for understanding disordered quantum systems and developing state transfer protocols with reasonable fidelity.

keyword: correlated disorder; Heisenberg spin chain; autocorrelation; disordered

Running title : Quantum Heisenberg Spin Chains with Inversely Linear Correlated Disorder

Academy Section : Physical Sciences

1 Introduction

The phenomenon of Anderson localization, first introduced by P. W. Anderson in 1958 [Anderson 1958], describes the suppression of electronic wave diffusion in a disordered medium due to quantum interference. In one-dimensional $1D$ systems, the presence of uncorrelated disorder leads to the exponential localization of all electronic states, independent of disorder strength [Abrahams *et al.* 1979]. However, the introduction of correlated disorder complicates the scenario, giving rise to novel localization phenomena. Correlated disorder introduces spatial correlations between the disorder potentials, thereby influencing the localization properties of electronic states in profound ways. For instance, long-range correlations can induce extended states even in 1D systems, which stands in contrast to the expectations from the theory of uncorrelated disorder [Izrailev & Krokhin 1999, Rodriguez *et al.* 2003]. The nature and extent of these correlations are critical in determining both the localization length and the overall transport characteristics of the system. Recent studies have examined the effects of various types of correlated disorder, such as power-law correlated disorder [Izrailev *et al.* 2012], Lorentzian-distributed disorder [Mourik *et al.* 2023], and random dimer models [Dunlap *et al.* 1990], on the localization behavior of 1D systems. These investigations have offered deeper insights into how correlations modify key parameters associated with localization, including the localization length and the structure of the localized states. A particularly interesting development is the interplay between correlated disorder and non-Hermitian effects, explored in recent works [Longhi 2019]. In these systems, localization properties are markedly altered, leading to phenomena such as the non-Hermitian skin effect [Yao & Wang 2018], where bulk states become localized at the system boundaries. Additionally, external fields or particle interactions in the presence of correlated disorder can further enrich the localization landscape [Luitz *et al.* 2015, Modak & Mukerjee 2015], either enhancing or diminishing localization, depending on the system's specific attributes.

The reduction of thermal conductivity in insulators and semiconductors through the incorporation of spatial correlations within intrinsic disorder has been extensively studied using large-scale simulations, involving tens of millions of atoms [Thébaud *et al.* 2023]. These simulations showed that isotropic long-range correlations in defect distributions could substantially reduce phonon lifetimes and thermal conductivity, potentially by an order of magnitude at room temperature. This research established a framework for modulating thermal transport via structural correlations and identified optimal correlation patterns for minimizing thermal conductivity. Experimental realizations of these structures for practical applications were also discussed. Furthermore, in [Yang *et al.* 2024], it was shown that correlated disorder critically affects photonic transport. Quasiperiodic lattices exhibit nearly ballistic transport, while amorphous lattices show partial transport disruption, and fully random lattices deviate entirely from ballistic behavior. The photon spreading coefficient was found to depend on the characteristic length scale of the disorder, offering a clear classification of disor-

der types in materials. Numerical studies in [Duthie *et al.* 2022] revealed that an unusual and robust multifractal regime emerges in a one-dimensional quantum chain with exponentially correlated disorder, beyond a threshold disorder strength. Below this threshold, mixed and extended regimes exist at weaker disorder strengths. In this multifractal regime, the states are uniformly spread across a continuous segment of the chain, with lengths that scale in a nontrivial manner with system size. This anomaly influences the system dynamics, enabling ballistic transport of a localized wavepacket, in contrast to the subdiffusive behavior typically observed in multifractal systems. A novel paradigm of dynamical quantum phase transitions driven by internal disorder potential correlations was proposed in [Khan *et al.* 2023], which explored anomalous phase transitions due to infinite disorder correlations and quench dynamics between random and pure Hamiltonians. Additionally, phase transitions involving a prequench white-noise potential and delocalization features in the correlated Anderson model were investigated. In [Neverov *et al.* 2024], the effects of correlated disorder on the superconducting properties of disordered superconductors were analyzed using an attractive Hubbard lattice Hamiltonian with point interactions, designed to model s-wave Cooper pairing. The study examined how spatial correlations in disorder influence the density of states and the superconducting coupling constant matrix elements. It was demonstrated that surface superconductivity can persist in the presence of weak to moderate bulk disorder [Bragança *et al.* 2024]. Interestingly, under moderate disorder conditions, the surface critical temperature may increase depending on the disorder's intensity and correlation characteristics.

The long-held belief that all states in 1D disordered systems with short-range hopping and uncorrelated potential are localized was challenged in [Lin & Gong 2024]. By coupling a disordered chain (with localized states) to a free chain (with extended states), distinct localization behaviors were observed in overlapped and non-overlapped regimes, without a phase transition. A significant suppression of localization occurred in the non-overlapped regime, influenced by the strength of inter-chain coupling and the energy shift between chains, suggesting localization lengths comparable to system sizes even under strong disorder. This was verified through extensive numerical simulations. Similarly, localization-delocalization transitions in double-chain models with long-range correlations were investigated in [Zhao *et al.* 2020]. The exact positions of mobility edges were identified, with results consistent with numerical transfer matrix methods. A second-order quantum phase transition due to inter-chain correlations in on-site energies was discovered, indicated by a critical exponent jump in localization length. Without inter-chain correlation, the critical exponent was determined by the chain with the weaker long-range correlation. Finally, the transfer of a magnon state across a quantum Heisenberg model with correlated disorder and random magnetic fields was examined in [Junior *et al.* 2023]. The disorder followed a power-law spectrum distribution, while the magnetic fields were uniformly random. Numerical analyses focused on the interplay between disorder and correlation in transferring the magnon state along the chain, eval-

uating transfer fidelity and end-to-end concurrence to identify conditions under which high-fidelity state transfer protocols are feasible despite the disorder.

In recent years, exploring entanglement as a tool for studying localization in disordered quantum chains has gained significant attention [Mohdeb et al. 2020, Lin & Chen 2023]. The role of entanglement measures, such as concurrence and entanglement entropy, has become crucial in characterizing quantum phases and understanding the transitions between localized and extended states in these systems. These works demonstrate how these measures provide insights into the impact of disorder correlations on quantum state transfer and localization, opening new avenues for analyzing quantum transport in disordered systems. The authors in ref. [Lin & Chen 2023] modifies a quantum algorithm for many-body localization (MBL) by adding a measurement on a quantum ancilla, enabling the determination of dynamics through both ensemble averages and quantum interference. The approach enhances dephasing and accelerates entanglement growth, significantly reducing saturation times in the deep MBL phase. Numerical simulations support these findings, showing entanglement enhancement even for smaller disorder strengths. This method provides a faster means to investigate long-time MBL behavior. The ref. [Mohdeb et al. 2020] explores entanglement measures, specifically concurrence and entanglement entropy (EE), in quantum spin chains with random long-range couplings decaying spatially as a power law. Using the strong disorder renormalization group (SDRG) method and numerical diagonalization, the work uncovers a critical behavior with logarithmic EE enhancement and power-law decay in concurrence, influenced by the coupling decay exponent α. It also identifies distinctions in results from SDRG, numerical diagonalization, and DMRG for varying α.

In this work, we present new results in the context of localization and quantum state transfer in models with correlated disorder. Specifically, we investigate the effects of correlated disorder on the quantum Heisenberg spin chain, where the exchange couplings between adjacent spins are modeled using a disordered distribution with an inverse linear correlation function, parameterized by γ. To ensure the spin-spin couplings adhere to this correlation structure, we employ the Cholesky decomposition method [Fritzsche et al. 2024]., which allows us to generate a correlated disorder with a desired covariance matrix. The Cholesky decomposition factorizes the correlation matrix into a product of a lower triangular matrix and its transpose, ensuring that the resulting disorder configuration maintains the prescribed correlation characteristics. This approach is particularly useful for generating large systems with correlated disorder, as it efficiently captures the spatial correlation between adjacent spins while adhering to the statistical properties dictated by the inverse linear correlation function. Our analysis begins with the autocorrelation function, which we use to examine how the parameter γ influences the decay behavior of correlations. This approach provides insight into how different levels of correlation affect the statistical properties of disorder in the spin chain. We then focus on the eigenstates of the Hamiltonian in the one-magnon subspace, analyzing the behavior of the participation ratio and the state transfer fidelity. The participation ratio cal-

culations shed light on the system's localization characteristics, revealing how correlated disorder impacts the spatial distribution and extent of the eigenstates. Using the eigenstates obtained through exact diagonalization, we compute the evolution operator to investigate the transfer of an initially localized spin state from one end of the chain to the opposite end, spanning approximately 100 sites. Our numerical calculations demonstrate the specific limits of disorder and correlation required to achieve maximized state transfer fidelity. These calculations provide valuable benchmarks for understanding the interplay between disorder and quantum transport, contributing to the broader field of research on correlated disordered systems.

2 Model and Formalism

We considered a disordered chain of N Heisenberg spins ($S = 1/2$). The Hamiltonian for this model was given by [Nunes *et al.* 2016, Kosevich & Gann 2013, de Moura et al. 2002, Evangelou & Katsanos 1992]:

$$\mathcal{H} = -\sum_{n=1}^{N} \left[J_n \vec{S}_n \cdot \vec{S}_{n+1} \right] \tag{1}$$

where J_n represents the exchange couplings connecting sites n and $n+1$. In our work, we considered J_n as a correlated disordered distribution with correlations between J_n and J_m defined by the function $C(r = |n-m|) = \frac{1}{1+\gamma r}$, where γ is a tunable parameter that controls the correlation strength. To generate the sequence J_n with this correlation, we employed the Cholesky decomposition method [Fritzsche *et al.* 2024]. The process began by constructing the covariance matrix C with elements $C_{nm} = C(|n-m|)$. This matrix was then decomposed using the Cholesky decomposition into the product of a lower triangular matrix L and its transpose, $C = LL^T$. Given a vector U of independent standard normal random variables, the correlated sequence Z_n was obtained as $Z_n = L \cdot U$. This ensures that the sequence Z_n has the desired correlations. After generating Z_n, we normalized it to have zero mean and unit variance, $\langle Z_n \rangle = 0$ and $\langle Z_n^2 \rangle - \langle Z_n \rangle^2 = 1$. The spin coupling distribution was therefore generated as $J_n = 2 + W \tanh(Z_n)$ where W is a tunable parameter that controls the strength of the correlation. The Cholesky decomposition is a useful method for generating correlated disorder however, for long chains (large N), this method can become inefficient and is not highly recommended. The primary limitation is that the Cholesky decomposition has a computational complexity of $O(N^3)$, making it increasingly slow and resource-intensive as the system size grows. We would like to emphasize that it is now experimentally possible to produce correlated disorder in various types of systems. For example, a recent study [Vynck *et al.* 2023] investigated a broad range of optical systems featuring various types of correlated disorder. In optical systems, several key techniques are used to study correlated disorder: Optical lattices create controllable disorder patterns via laser interference. Disordered photonic crystals

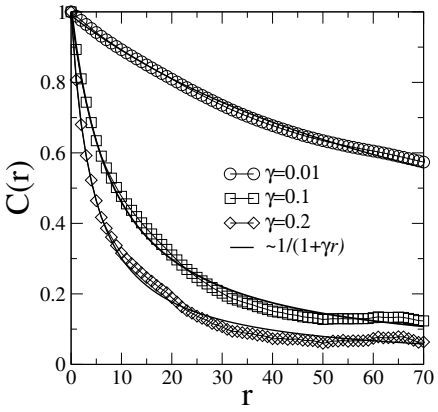

Figure 1: Autocorrelation function $C(r)$ versus $r = |i - j|$ and γ. The figure shows different decay behaviors depending on the value of γ.

and waveguide arrays introduce variations in dielectric properties or waveguide parameters to explore light propagation and localization. Random media experiments involve adding scatterers to study wave scattering, while metamaterials with engineered disorder reveal novel optical phenomena. Nonlinear optical systems provide insights into how disorder affects nonlinear interactions. Thus, it is now experimentally feasible to generate various forms of correlated disorder, including those with unusual correlation functions. We will explore now the behavior of J_n and its dependence on the correlation parameter γ. The autocorrelation function $C(r) = [\langle J_n J_{n+r}\rangle - \langle J_n\rangle\langle J_{n+r}\rangle]/[\langle J_n^2\rangle - \langle J_n\rangle^2]$ was computed as a function of r for several values of γ. The main results of these calculations can be found in Fig. 1. We observed that for $\gamma \to \infty$, the function $C(r)$ decayed rapidly, indicating a short-range correlated disorder. As γ decreased, the correlations became longer-ranged, affecting the physical properties of the system.

We were interested in studying the one-magnon subspace of this Hamiltonian. The ground state $|0\rangle$ of the system contained all spins pointing in the same direction. If a spin deviation occurred at a site n, this excited state was described by $|n\rangle = S_n^+|0\rangle$. The eigenstates of the Hamiltonian were therefore given by $|\Psi^j\rangle = \sum_{n=1}^{N} f_n^j|n\rangle$, where the coefficients f_n^j satisfied the equation [Nunes *et al.* 2016, Evangelou & Katsanos 1992]:

$$(J_n + J_{n-1})f_n^j - J_n f_{n+1}^j - J_{n-1}f_{n-1}^j = 2E_j f_n^j \tag{2}$$

We express the previous equation in matrix form and use exact diagonalization to solve the disordered Heisenberg chain. This method allows us to compute the eigenvalues and eigenvectors of the Hamiltonian matrix, which are essential for analyzing the system's behavior. By obtaining the eigenstates, we can calculate various system properties, including the density of states (DOS), de-

noted as $DOS(E) = \sum_j \delta(E - E_j)$*, where* $\{E_j\}$ *represents the eigenvalues. We can also calculate the participation ratio, which measures the spread of the wave function across the Hilbert space of the system. The participation ratio is defined by* $P_j = \left[\sum_{n=1}^{N} |f_n^j|^4\right]^{-1}$*. It is important to note that* P_j *remains constant for localized states and is proportional to* N *for extended states (source: [Izrailev et al. 2012]). In general, calculations of the participation ratio require many averages (typically 200 to 400 samples, or sometimes even more). Therefore, our study did not focus directly on the participation* P_j *of each eigenvalue. Instead, we used different samples to calculate an average participation ratio,* $\langle P \rangle$*. Specifically, for a given energy* E*, the average* $\langle \cdot \rangle$ *was computed using all data obtained within a small energy window, i.e., considering all the eigenvalues in the region* $[E - \delta E/2, E + \delta E/2]$ *with* $\delta E \approx 0.05$*.*

The efficiency of quantum state transfer in this system is studied by adding the terms $-g\vec{S}_0 \cdot \vec{S}_1 + h_0\vec{S}_0$ *and* $-g\vec{S}_N \cdot \vec{S}_{N+1} + h_{N+1}\vec{S}_{N+1}$ *to the initial Hamiltonian (eq. 1). Here, the parameter* g *represents the coupling between the additional spins and the system, while* h_0 *and* h_{N+1} *are external magnetic fields that we adjust to ensure the diagonal energy terms for spins* 0 *and* $N + 1$ *match a target energy* E*. To investigate the quantum state transfer from spin* 0 *to spin* $N + 1$*, we diagonalize the complete Hamiltonian, now composed of spin* 0*, the channel with* N *spins, and the final spin* $N + 1$*. In this context, the model defined in eq. 1 with* N *spins effectively functions as a channel connecting spin* 0 *to spin* $N + 1$*. We stress that in the context of quantum state transfer, the spins* 0 *and* $N + 1$ *added to the model serve as the source* S *and the receiver* R *, respectively, where spin* 0 *acts as the source* S *and spin* $N + 1$ *acts as the receiver* R*. Once this modified Hamiltonian, denoted* H_{QST}*, is diagonalized, we compute the time evolution operator* $e^{-iH_{QST}t}$*, which governs the system's dynamics. This operator is used to evolve the state from the initial configuration,* $|\Psi(t = 0)\rangle = \sum_{n=0}^{N+1} f_n(t = 0)|n\rangle$*, with* $f_n(t = 0) = \delta_{n,0}$*, to the final state. The efficiency of the quantum state transfer is quantified using the fidelity function* $F(t)$*, which measures the overlap between the initial and final states. Specifically, we use the expression* $F(t) = \frac{1}{2} + \frac{|f_{N+1}(t)|}{3} + \frac{|f_{N+1}(t)|^2}{6}$ *to assess the success of the state transfer [Bose 2003]. The maximum fidelity,* F_{max}*, is determined as the highest value of* $F(t)$ *over the time interval* $[10^5, 10^6]$*.*

3 Results

In this section, we present numerical calculations to investigate the behavior of the density of states ($DOS(E)$), participation ratio $\langle P \rangle(E)$, and fidelity F_{max} in a Heisenberg model with inverse linear correlations in the spin-spin coupling. The density of states ($DOS(E)$) and the participation ratio are analyzed using the exact diagonalization of the Hamiltonian (eq. 1). The fidelity is computed through the temporal evolution operator, obtained by diagonalizing the modified Hamiltonian of the full system, which includes the boundary spins (0 and $N + 1$) and the N internal spins as described in equation 1. These

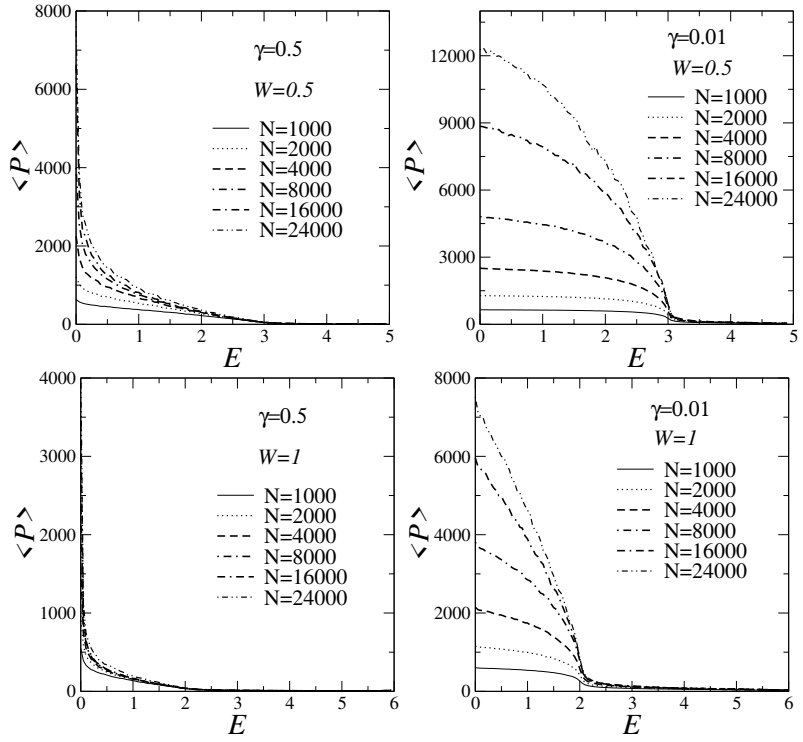

Figure 2: Participation ratio $\langle P \rangle$ as a function of system size N for $\gamma = 0.01$ and 0.5 with $W = 0.5$ and 1. For $\gamma = 0.5$, the ratio shows minimal dependence on N, indicating localization, while for $\gamma = 0.01$, it increases with N, suggesting a possible transition to extended states.

methods allow us to explore the system's behavior across various disorder parameters and system sizes. In our initial analysis, we examine the behavior of the participation ratio $\langle P \rangle(E)$ as a function of energy E for various system sizes N and two different values of the parameter γ. We consider system sizes $N = 1000, 2000, 4000, 8000, 16000$, and 24000, with γ set to 0.01 and 0.5, and $W = 0.5$ and $W = 1$. The participation ratio is a key quantity for understanding localization in disordered systems, reflecting the spatial extent of the wavefunctions. For $\gamma = 0.5$, the participation ratio for $E > 0$ shows a relatively weak dependence on the system size N, suggesting a localized phase where wavefunctions are spatially confined. As N increases, the participation ratio remains relatively constant, indicating that the localization length is roughly independent of system size. In contrast, for $\gamma = 0.01$, the participation ratio shows significant dependence on N, particularly in the low-energy region. The increase in $\langle P \rangle(E)$ with N suggests a potential transition to extended states, though this may be influenced by finite-size effects. Further investigation is

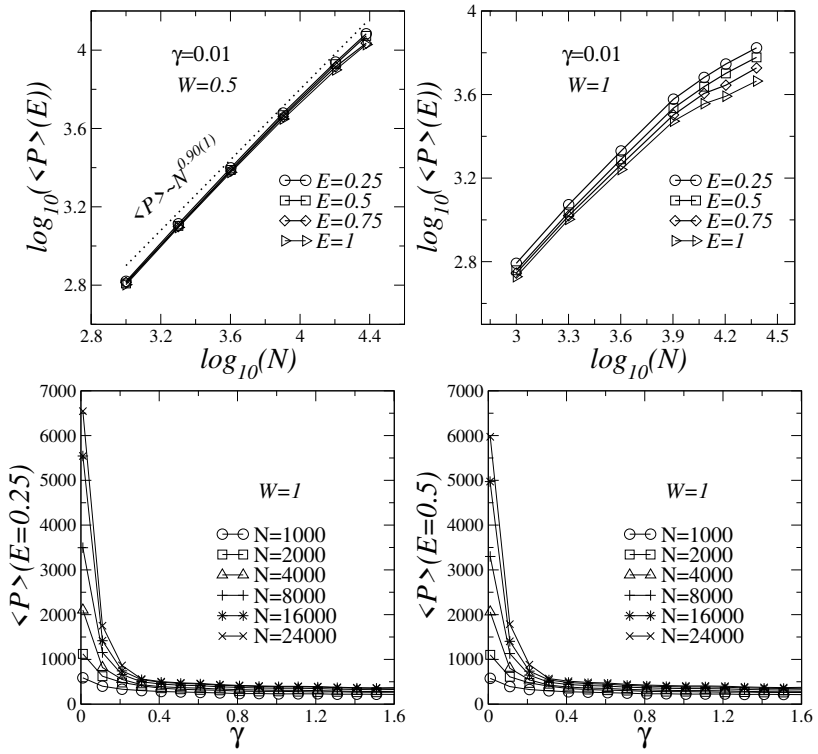

Figure 3: (a-b) Participation ratio $\langle P\rangle$ versus system size N for various disorder strengths W and energies E. The data shows strong localization at $W = 0.5$ and $E = 0.25$ with $\langle P\rangle \sim N^{0.90}$, and saturation at $W = 1$, indicating robust localization. (c-d) Participation ratio $\langle P\rangle(E)$ versus disorder parameter γ for $E = 0.25$ and 0.5. For $\gamma > 0$, $\langle P\rangle$ remains strongly localized, while for γ close to zero, it increases with $N^{0.9}$, but still indicates localization.

needed to determine if this trend reflects a true delocalization transition or if it is merely an artifact of finite-size effects. Analyzing the scaling of $\langle P\rangle(E)$ with N in more detail will be crucial to understanding the system's behavior.

We present figures (see fig. 2) showing the participation ratio $\langle P\rangle$ as a function of system size N for $\gamma = 0.01$ with $W = 0.5$, $W = 1$, and $E = 0.25, 0.5, 0.75, 1$. For $W = 0.5$ and low energy, particularly $E = 0.25$, the participation ratio follows a power law $\langle P\rangle \sim N^{0.90}$, indicating strong localization in the large N limit. For $W = 1$, the participation ratio shows signs of saturation as N increases, confirming localization in the thermodynamic limit. These results suggest that localization persists for both disorder strengths, with $W = 1$ showing clearer evidence of saturation.

We also examine in fig. 3 $\langle P\rangle(E)$ as a function of the disorder parameter γ for

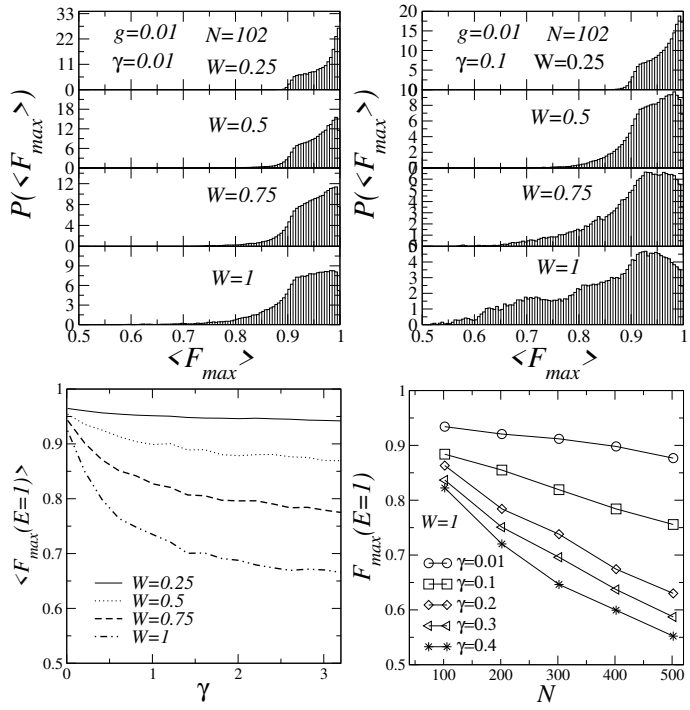

Figure 4: (a-b)Probability distribution of F_{max} for $E = 1$ and varying disorder parameters γ. For $\gamma = 0.1$, F_{max} is predominantly less than 1, indicating limited state transfer, while for $\gamma = 0.01$, F_{max} is closer to 1, suggesting enhanced state transfer. c) Fidelity F_{max} as a function of disorder strength W for $E = 1$ and varying γ. At $W = 0.25$ and $W = 0.5$, the fidelity remains high for moderate γ, but decreases for $W > 0.5$, even for $\gamma < 1$, indicating reduced state transfer.

$E = 0.25$ and $E = 0.5$, with system sizes ranging from $N = 1000$ to $N = 24000$. For $\gamma > 0$, the participation ratio does not show substantial growth with N, indicating Anderson localization. For γ values close to zero, the participation ratio increases approximately as $N^{0.9}$, reinforcing the localization observed in previous results.

Regarding quantum state transfer, we consider a system of $N = 102$ spins with energy $E = 1$. In the quantum state transfer experiment, we introduced two additional spins to the previously studied model: one at position $n = 0$, acting as the source for the initial quantum state, and a receiver spin at the far right of the chain. Thus, the system now includes these two additional spins. For our study, we set $N = 102$, where the two additional spins are combined with the internal chain of 100 spins, identical to those described by the Hamiltonian in equation 1. The external fields h_0 and h_{N+1} are adjusted such that the diagonal energy terms associated with spins 0 and $N + 1$ match the energy E.

The probability distribution of F_{max} as a function of F_{max} for $E = 1$ and varying γ shows that, for $\gamma = 0.1$, a large portion of the distribution is concentrated at $F_{max} \ll 1$, indicating limited quantum state transfer. However, for $\gamma = 0.01$ and low energies, the distribution shifts closer to $F_{max} \approx 1$, suggesting enhanced state transfer and potential delocalization. The figure 4 illustrates F_{max} at $E = 1$ as a function of γ for different disorder strengths: $W = 0.25$, 0.5, 0.75, and 1. For $W = 0.25$ and $W = 0.5$, the fidelity remains near 0.9, indicating efficient state transfer. However, for $W > 0.5$, even when $\gamma < 1$, the fidelity begins to deviate from 1, indicating reduced state transfer. As γ approaches zero, the fidelity F_{max} approaches 1 even in the presence of strong disorder, highlighting enhanced state transfer at low γ. It is important to note that these state transfer experiments were conducted at $E = 1$, higher than the uniform mode at $E = 0$, to investigate the impact of disorder correlations on quantum state transfer in regions away from very low energy, where disorder effects are less pronounced. We also performed quantum state transfer experiments for slightly larger N values $(202 - 502)$, and the results are qualitatively the same: (i) low fidelity for $\gamma > 0$ and non-zero energy E, and (ii) fidelity close to 1 as $\gamma \to 0$ and in the low-energy region. For all values of γ considered, we can observe a slight decrease in F_{max} as N increases. However, for very small γ (for example, 0.01 and 0.1), despite this decrease, we still find a reasonable level of fidelity in the quantum state transfer process.

4 Summary

In this study, we have explored the behavior of a disordered 1D system with non-reciprocal disorder, focusing on the participation ratio $\langle P \rangle$ and its dependence on energy E, system size N, and disorder strength parameter γ. Our analysis revealed distinct phases based on the value of γ. For higher values of γ, the system exhibits localization, as indicated by a participation ratio that becomes independent of system size for $E > 0$. This suggests a localized phase where wavefunctions remain spatially confined, with the localization length not depending significantly on N. On the other hand, for smaller values of γ, the participation ratio increases with system size, particularly at low energies, suggesting a potential transition to extended states. This behavior raises the possibility of a delocalization transition, although finite-size effects need to be further investigated to confirm this trend. The scaling of the participation ratio with system size is a key tool in understanding the nature of these transitions and requires further detailed analysis. The study also examined the effect of disorder on quantum state transfer in a chain of $N = 102$ spins, where two additional boundary spins were introduced to control the energy levels at both ends of the chain. The results showed that the fidelity of quantum state transfer, measured by F_{max}, exhibits strong dependence on γ. For $\gamma = 0.1$, a large portion of the fidelity distribution was concentrated at low values ($F_{max} \ll 1$), indicating poor state transfer. However, for smaller values of γ (e.g., 0.01), the fidelity increased significantly, suggesting enhanced state transfer and potentially indicating de-

localization. The results also demonstrated that disorder strength W plays a critical role in the efficiency of state transfer, with higher disorder values leading to reduced fidelity.

The results of this study are significant in understanding the interplay between disorder, system size, and the localization-delocalization transition in disordered quantum systems. The transition between localized and extended states is a central phenomenon in condensed matter physics, particularly in systems where disorder plays a crucial role in the system's properties. The observation that the participation ratio remains constant for larger systems at higher γ and increases with system size at lower γ is consistent with the expected behavior of Anderson localization in disordered systems. These findings are particularly relevant for quantum information processing and quantum state transfer, as they suggest that minimizing disorder could be a strategy for enhancing quantum coherence and fidelity of information transfer. The enhanced state transfer observed at lower γ could be useful in the development of quantum communication protocols, where maintaining high fidelity is essential for efficient data transmission. Our study also contributes to the ongoing research on the role of disorder in quantum systems, offering new perspectives on how non-reciprocal disorder impacts quantum state transfer and the localization behavior.

Furthermore, our results open several exciting directions for future research. One promising avenue is to extend the study of non-reciprocal disorder to higher-dimensional systems, which could offer insights into the robustness of the delocalization transition in more complex geometries. Additionally, a more comprehensive exploration of the finite-size effects and their impact on the localization transition would help in better understanding the scaling behavior of quantum systems in the presence of disorder. Finally, experimental realizations of disordered quantum systems, such as those based on ultracold atoms or superconducting qubits, could offer an experimental platform to test the theoretical predictions made here, allowing for a deeper understanding of the role of disorder in quantum state transfer and other quantum phenomena.

In conclusion, this work provides significant contributions to our understanding of the complex interplay between disorder, system size, and quantum state transfer. The results suggest that minimizing disorder may be crucial in enhancing quantum coherence and improving the efficiency of state transfer, which is vital for the development of future quantum technologies. With continued research in this area, we can expect further advances in our understanding of disordered quantum systems, offering new insights into localization phenomena and the transmission of quantum information in disordered media.

5 Acknowledgments

This work was supported by CNPq, CNPq-Rede Nanobioestruturas, CAPES, FINEP (Federal Brazilian Agencies), FAPEAL (Alagoas State Agency), and FACEPE (Pernambuco State Agency).

References

[Abrahams *et al.* 1979] ABRAHAMS E, ANDERSON PW, LICCIARDELLO DC & RAMAKRISHNAN TV 1979. Scaling Theory of Localization: Absence of Quantum Diffusion in Two Dimensions. Phys. Rev. Lett. 42: 673-676.

[Anderson 1958] ANDERSON PW 1958. Absence of Diffusion in Certain Random Lattices. Phys. Rev. 109: 1492-1505.

[Bragança *et al.* 2024] de BRAGANÇA RH, de MORAES LMT, ROMAGUERA ARdeC, AGUIAR JA & CROITORU MD 2024. Impact of Correlated Disorder on Surface Superconductivity: Revealing the Robustness of the Surface Ordering Effect. The Journal of Physical Chemistry Letters 15: 2573-2579.

[Bose 2003] BOSE S 2003. Quantum Communication through an Unmodulated Spin Chain. Phys. Rev. Lett. 91: 207901.

[de Moura et al. 2002] de MOURA FABF, COUTINHO-FILHO MD, RAPOSO EP & LYRA ML. 2002. Delocalization and spin-wave dynamics in ferromagnetic chains with long-range correlated random exchange. Phys. Lett. B 66: 014418.

[Dunlap *et al.* 1990] DUNLAP DH, WU HL & PHILLIPS PW 1990. Absence of Localization in a Random Dimer Model. Phys. Rev. Lett. 65: 88-91.

[Duthie *et al.* 2022] DUTHIE A, ROY S & LOGAN DE 2022. Anomalous multifractality in quantum chains with strongly correlated disorder. Phys. Rev. B 106: L020201.

[Evangelou & Katsanos 1992] EVANGELOU SN & KATSANOS DE. 1992. Super-diffusion in random chains with correlated disorder. Phys. Lett. A 164: 456.

[Izrailev & Krokhin 1999] IZRAILEV FM & KROKHIN AA 1999. Anomalous Localization in Low-Dimensional Systems with Correlated Disorder. Phys. Rev. Lett. 82: 4062-4065.

[Izrailev *et al.* 2012] IZRAILEV FM, KROKHIN AA & MAKAROV NM 2012. Anomalous localization in low-dimensional systems with correlated disorder. Physics Reports 512: 125-254.

[Izrailev *et al.* 2012] IZRAILEV FM, MAKAROV NM & TORRES-HERRERA EJ 2012. Anderson Localization in Low-Dimensional Systems with Long-Range Correlated Disorder. Physica B: Condensed Matter 407: 2277-2281.

[Junior *et al.* 2023] JUNIOR MSS, de LIMA WVP, TEIXEIRA VA, da FONSECA DB, MORAES F, BARBOSA ALR, ALMEIDA GMA & de MOURA FABF 2023. Magnon state transfer in chains with correlated disorder. Journal of Magnetism and Magnetic Materials 579: 170880.

[Khan *et al.* 2023] KHAN NA, WANG P, JAN M & XIANLONG G 2023. Anomalous correlation-induced dynamical phase transitions. Sci Rep 13: 9470.

[Kosevich & Gann 2013] KOSEVICH YA & GANN VV 2013. Magnon localization and Bloch oscillations in finite Heisenberg spin chains in an inhomogeneous magnetic field. J. Phys.: Condens. Matter 25: 246002.

[Lin & Gong 2024] LIN X & GONG M 2024. Fate of localization in a coupled free chain and a disordered chain. Phys. Rev. A. 109: 033310.

[Longhi 2019] LONGHI 2019. Topological Phase Transition in Non-Hermitian Quasicrystals. Phys. Rev. Lett. 122: 237601.

[Luitz *et al.* 2015] LUITZ DJ, LAFLORENCIE N & ALET F 2015. Many-Body Localization Edge in the Random-Field Heisenberg Chain. Phys. Rev. B 91: 081103.

[Modak & Mukerjee 2015] MODAK R & MUKERJEE S 2015. Many-Body Localization in the Presence of a Single-Particle Mobility Edge. Phys. Rev. Lett. 115: 230401.

[Mourik *et al.* 2023] MOURIK V, NADJ-PERGE S, FROLOV SM, PRIBIAG VS & KOUWENHOVEN LP 2023. Disorder-Induced Localization in Topological Superconductors. Nat. Phys. 19: 243-248.

[Neverov *et al.* 2024] NEVEROV VD, LUKYANOV AE, KRASAVIN AV, VAGOV A, LVOV BG & CROITORU MD 2024. Exploring disorder correlations in superconducting systems: spectroscopic insights and matrix element effects. Beilstein J. Nanotechnol. 15: 199-206.

[Nunes *et al.* 2016] NUNES DM, NETO AR & de MOURA FABF 2016. Coherent magnon dynamics in ferromagnetic models with nonuniform magnetic field and correlated disorder. Journal of Magnetism and Magnetic Materials 410: 165-170.

[Rodriguez *et al.* 2003] RODRIGUEZ A, MALYSHEV VA, SIERRA G, MARTIN-DELGADO MA, RODRIGUEZ-LAGUNA J & DOMINGUEZ-ADAME F 2003. Anderson Transition in Low-Dimensional Disordered Systems Driven by Long-Range Correlated Disorder. Phys. Rev. Lett. 90: 027404.

[Thébaud *et al.* 2023] THÉBAUD S, LINDSAY L & BERLIJN T 2023. Breaking Rayleigh's Law with Spatially Correlated Disorder to Control Phonon Transport. Phys. Rev. Lett. 131: 026301.

[Vynck *et al.* 2023] VYNCK K, PIERRAT R, CARMINATI R, FROUFE-PÉREZ LS, SCHEFFOLD F, SAPIENZA R, VIGNOLINI S & SÁENZ JJ 2023. Light in correlated disordered media. Rev. Mod. Phys. 95: 045003.

[Yang *et al.* 2024] YANG Y-Y, CHANG YJ, LU Y-H, ZHU K-D & JIN X-M 2024. Probing Structural Correlated Disorder with Photonic Transport. ACS Photonics 11: 1024-1030.

[Yao & Wang 2018] YAO S & WANG Z 2018. Edge States and Topological Invariants of Non-Hermitian Systems. Phys. Rev. Lett. 121: 086803.

[Zhao *et al.* 2020] ZHAO Y, ZHANG W & YAN X-G 2020. Mobility edges and critical exponents in the disordered double chains with long-range correlation. Physica E: Low-dimensional Systems and Nanostructures 121: 114098.

[Mohdeb *et al.* 2020] MOHDEB Y, VAHEDI J, MOURE N, ROSHANI A, LEE H-Y, BHATT R N, KETTEMANN S & HAAS S 2020. Entanglement properties of disordered quantum spin chains with long-range antiferromagnetic interactions. Phys. Rev. B 102: 214201. DOI: 10.1103/PhysRevB.102.214201.

[Lin & Chen 2023] Lin, J.-D., & Chen, Y.-N. 2023. Boosting entanglement growth of many-body localization by superpositions of disorder. *Phys. Rev. A*, **108**(2): 022203. DOI: 10.1103/PhysRevA.108.022203.

[Fritzsche *et al.* 2024] Fritzsche, N., Ott, F., Hevisov, D., Reitzle, D., & Kienle, A. 2024. Theoretical Investigation of the Influence of Correlated Electric Fields on Wavefront Shaping. *Photonics*, **11**, 797. DOI: 10.3390/photonics11090797.